Supplementary information to "Conformational dynamics of CYP3A4 demonstrate the important role of Arg212 coupled with the opening of ingress, egress and solvent channels to dehydrogenation of 4-hydroxy-tamoxifen" by K. Shahrokh, T. E. Cheatham III and G. S. Yost submitted to Biochimica et Biophysica Acta. (2012).

Figure 1: 2D RMSD plots of five independent MD trajectories (m1-m5) of PDB ID:1TQN. The X and Y-axis represent ~40 ns of MD with the color ranging from low RMSD at blue (0 Å) through green (~1.5 Å) to higher RMSd going from yellow (~2 Å) to red (< 3 Å).

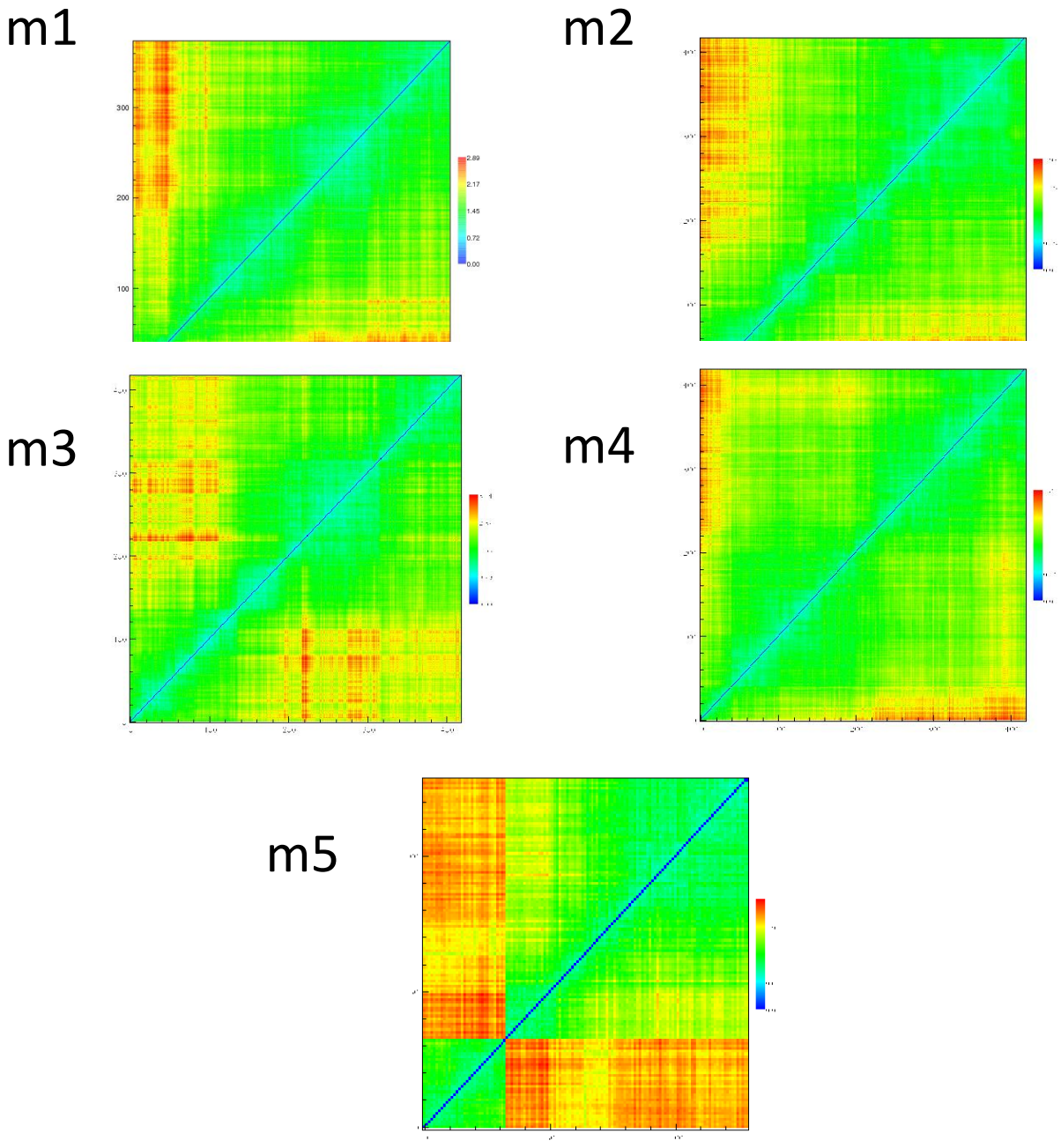

Supplementary Figure 2: Difference in HF versus B3LYP energies for dihedral scan of MTOXY tail (C5-C4-O11-C12)

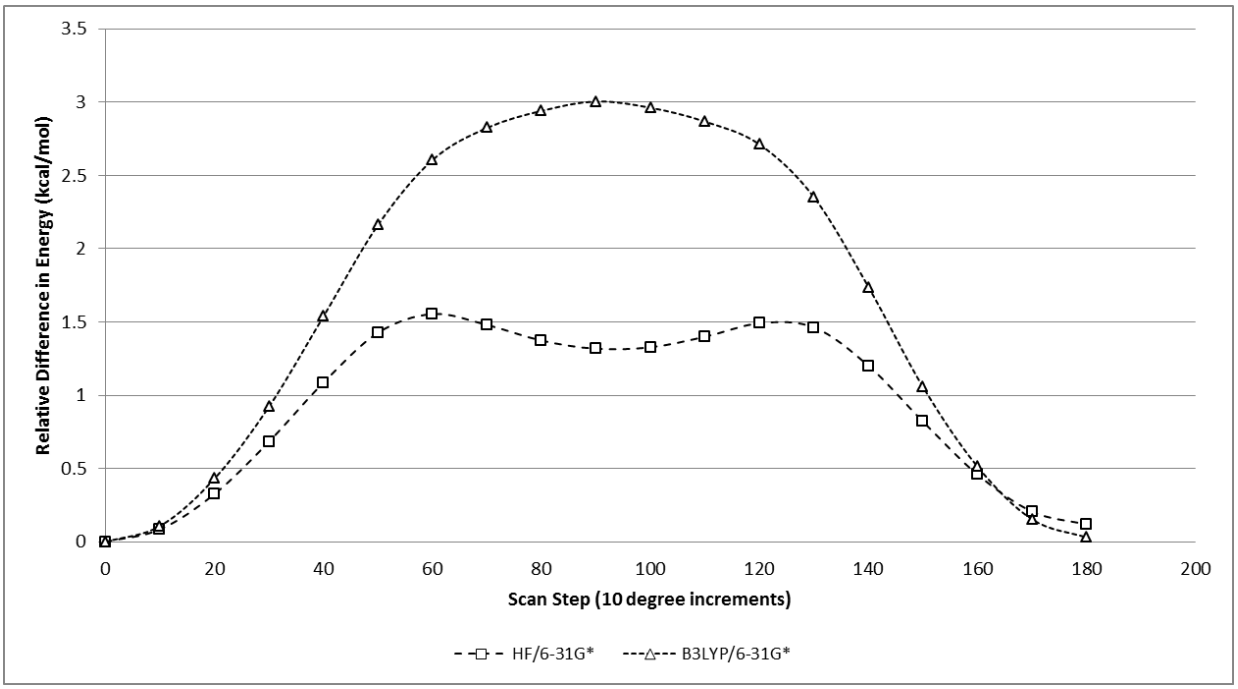

Supplementary information Figure 3: Structures and numbering scheme of training set for ethyl (C7-C8-C11-C12) dihedral scans in relation to each ring system.

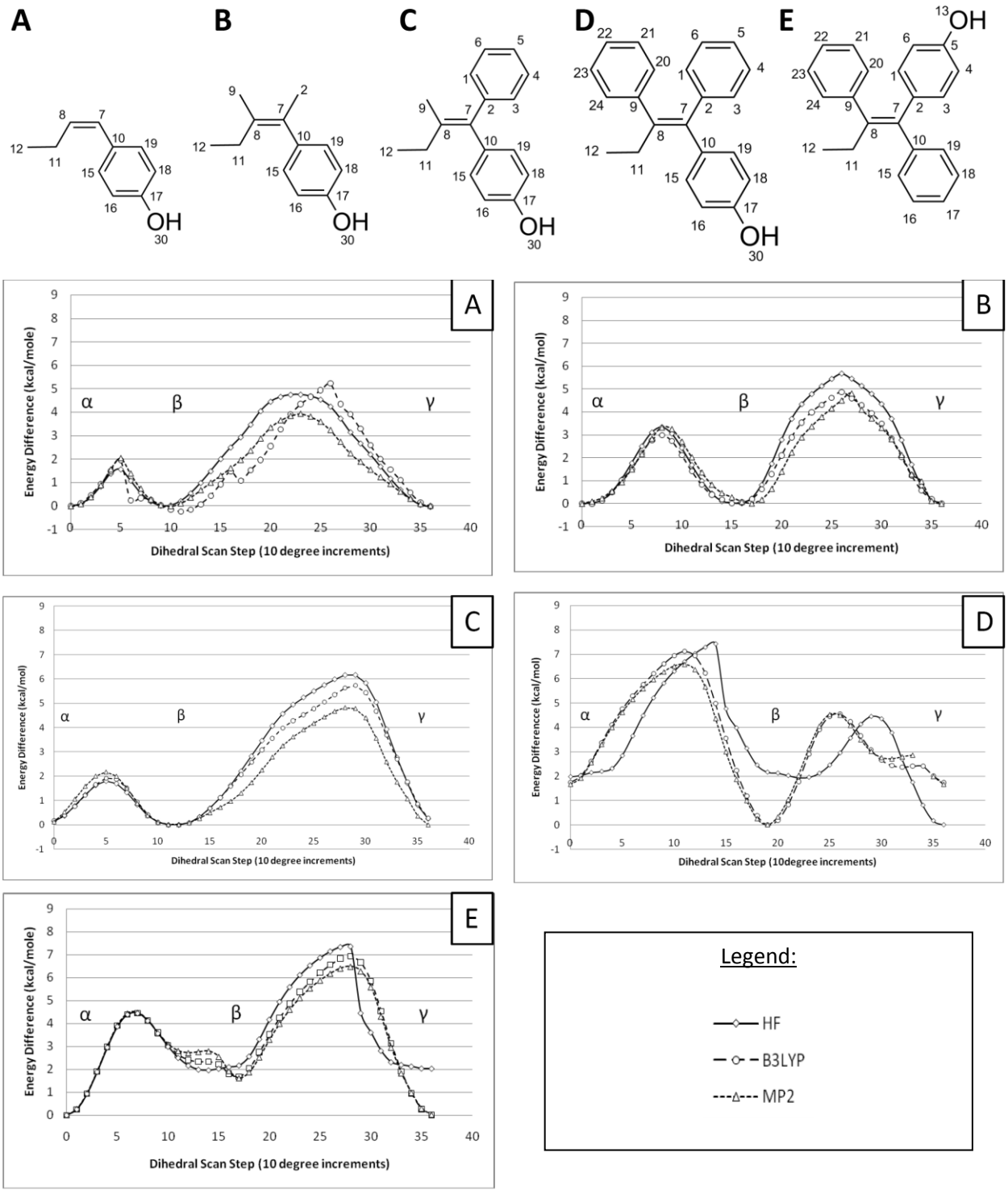

Supplementary information Figure 4: Ratio of Autodock3 binding modes supportive of observed metabolism of 4-hydroxy-tamoxifen reaction mechanisms alpha-hydroxylation (α-OH), dehydrogenation modes 1 & 2 (dH1 & dH2), N-demethylation (NdM) and non-productive and/or ambiguous modes (Non) with CYP3A4 (A) molecular dynamics refined m1-m5, experimentally derived x-ray (B) PDB ID: 1W0E, (C) PDB ID: 1TQN refined with quantum mechanics based heme parameters for resting high-spin (ic6) and Compound-I (cpdi) with (wq) and without (00) RESP charges assigned to the heme. Statistically significant differences are indicated with symbols: †, ‡ and * and differences are explained directly below each graph. Charge state of 4-hydroxy-tamoxifen is denoted as foht=neutral and fohtq=+1.

(A)

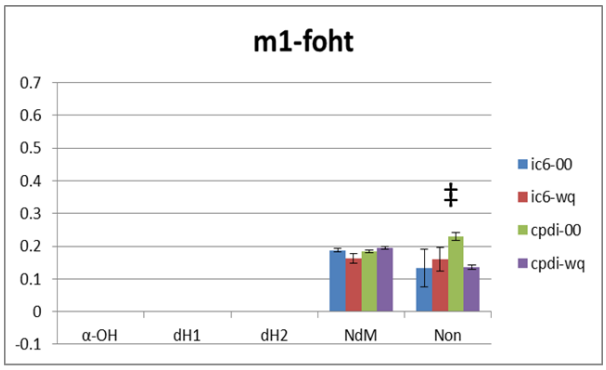

(‡) Non: cpdi-00 different from cpdi-wq

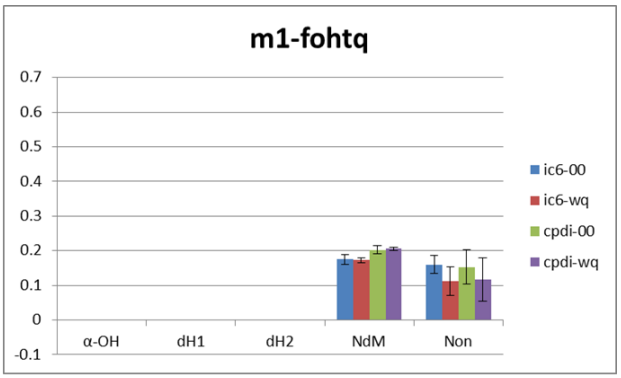

No significant differences between any of the results

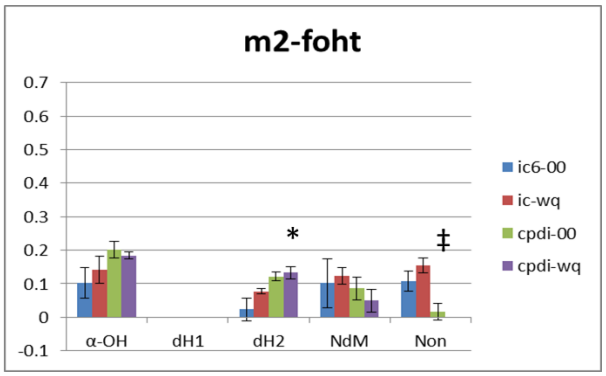

(*) dH2: ic6-00 from both cpdi's
(‡) Non: both ic6's from both cpdi's

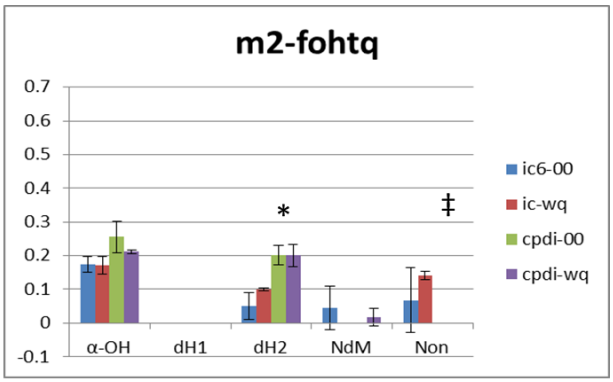

(*) dH2: ic6-00 from both cpdi's
(‡) Non: both ic6's from both cpdi's

(A)

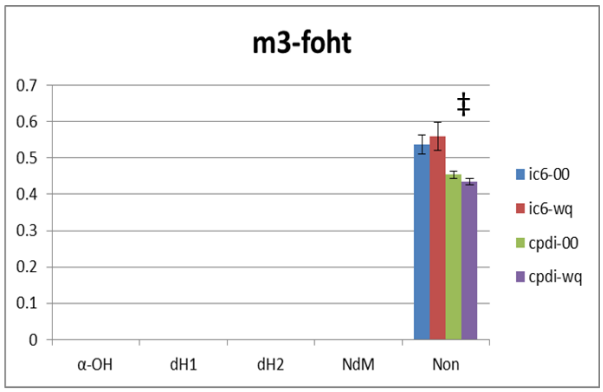

(‡) Non: both ic6's from both cpdi's

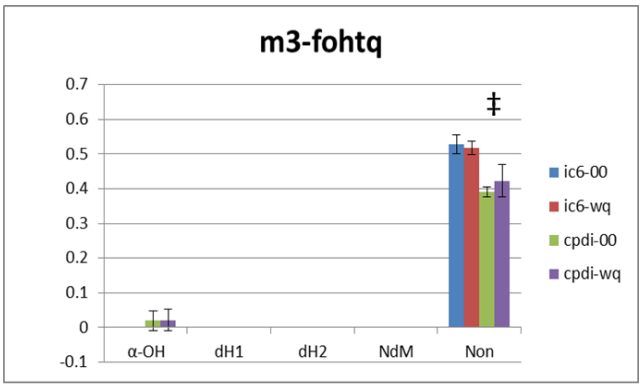

(‡) Non: both ic6's from both cpdi's

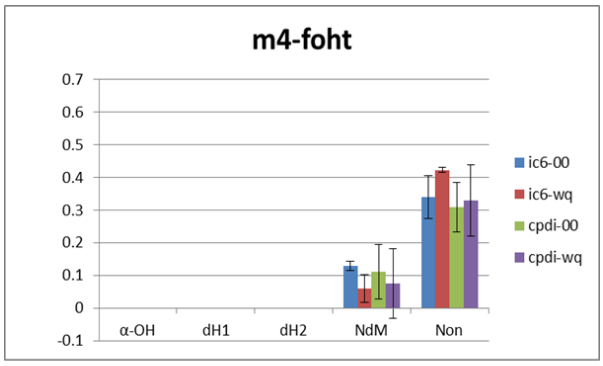

No significant differences between any of the results

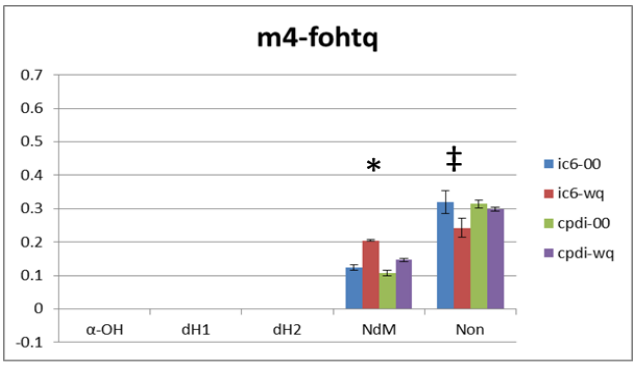

(*) NdM: ic6-wq from all the rest, ic6-00 from cpdi-wq, and cpdi-00 from cpdi-wq.
(‡) Non: ic6-00 from ic6-wq

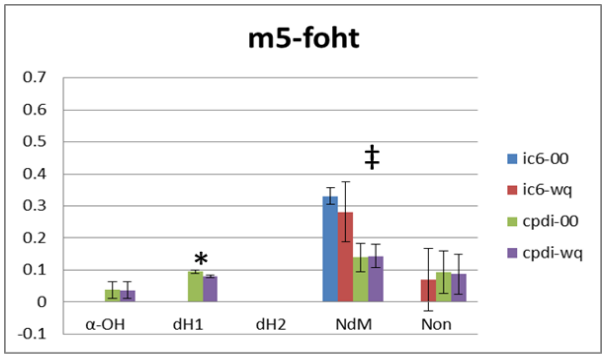

(*) dH1: both ic6's from both cpdi's
(‡) NdM: both ic6's from both cpdi's

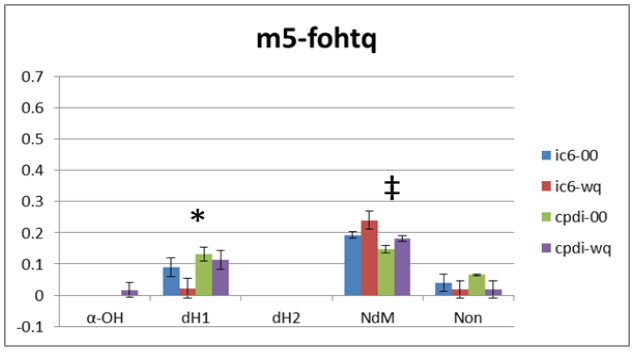

(*) dH1: ic6-wq from cpdi-00
(‡) NdM: ic6-wq from both cpdi's

(B)

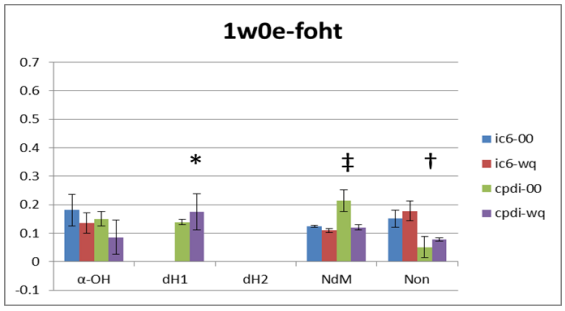

(*) dH1: both ic6's from both cpdi's
(‡) NdM: cpdi-00 from all the rest
(†) Non: both ic6's from cpdi-00 and ic6-wq from cpdi-wq

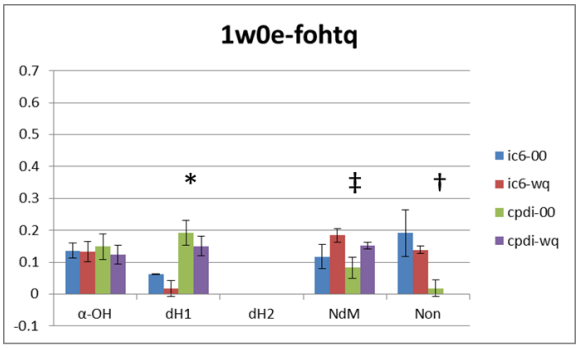

(*) dH1both ic6's from both cpdi's
(‡) NdM: ic6-wq from cpdi-00
(†) Non: ic6-00 from both cpdi's and ic6-wq from cpdi-wq

(C)

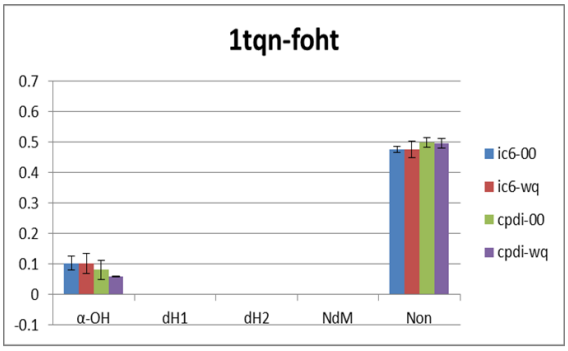

No significant differences between any of the results

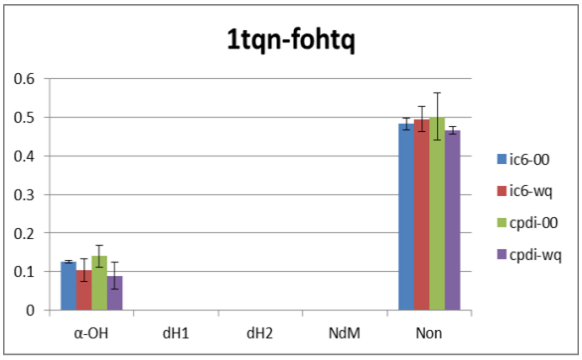

No significant differences between any of the results

Supplementary information Table 1: Mulliken atomic spin densities of key atoms for (i) four conformations (A-D) of open-shell intermediate first cationic intermediate of 4-dehydogenation with average values and standard deviation at each atom for all four conformations are given; (ii) for the A conformation of 4-hydroxytamoxifen three neutral radical intermediate species. For species formed from aliphathic hydrogen atom (H9 a/b) an average value (Avg C9) and atandard deviation (St Dev C9) is provided. Values for the radical formed from abstraction of the hydroxyl hydrogen atom are indicated (=O). Energy differences are in units of kcal/mol

(i)

FOHT Cat1	A	B	C	D	Average	St Dev
C7	0.04	0.06	0.06	0.04	0.05	0.01
C8	0.33	0.35	0.34	0.33	0.34	0.01
C9	-0.02	-0.02	-0.02	-0.02	-0.02	0.00
H9a	0.02	0.00	0.01	0.00	0.01	0.01
H9b	0.00	0.01	0.00	0.02	0.01	0.01
C10	0.02	0.02	0.02	0.02	0.02	0.00
O29	0.03	0.02	0.02	0.03	0.02	0.00
C26	0.13	0.15	0.15	0.13	0.14	0.01
H26a	-0.01	-0.01	-0.01	-0.01	-0.01	0.00
C12	0.00	0.00	0.00	0.00	0.00	0.00
C13	0.00	0.00	0.00	0.00	0.00	0.00
H29a	0.00	0.00	0.00	0.00	0.00	0.00
Energy Diff	0.00	0.25	0.51	0.05		

(ii)

FOHT Neu	H9a	H9b	Avg C9	St Dev C9	=O
C7	0.64	0.62	0.64	0.00	-0.12
C8	-0.15	-0.20	-0.15	0.00	0.19
C9	0.23	0.37	0.23	0.00	-0.01
H9a		-0.02	-0.02	0.00	0.01
H9b	-0.01		-0.01	0.00	0.00
C10	-0.02	-0.03	-0.02	0.00	0.01
O29	0.02	0.02	0.02	0.00	0.37
C26	-0.01	-0.01	-0.01	0.00	0.02
H22a	0.00	0.00	0.00	0.00	0.00
C25	0.00	0.00	0.00	0.00	0.00
C26	0.00	0.00	0.00	0.00	0.00
H30a	0.00	0.00			
Energy Diff	0.06	0.27			0.00

Supporting information Table 2: Dihedrals (in degrees) of the test set for ethyl scans at their energy minima: alpha, beta and gamma defined in supplementary information figure 3 above.

	α			β			γ		
A	HF	B3LYP	MP2	HF	B3LYP	MP2	HF	B3LYP	MP2
C7-C8-C11-C12	132.7	109.9	131.3	-137.3	-140.1	-128.7	132.7	109.9	-73.3
C8-C7-C10-C19	137.0	147.4	-137.4	138.4	150.3	-45.9	45.8	-34.9	-137.4
B									
C7-C8-C11-C12	100.4	100.4	95.9	-109.6	-109.6	-94.1	100.4	100.4	95.9
C8-C7-C10-C19	-90.2	-83.6	-92.0	-89.8	-111.2	-88.4	-90.2	-86.0	-91.9
C									
C7-C8-C11-C12	-128.9	-129.6	-126.6	121.1	120.4	113.4	-128.9	-129.6	-126.6
C8-C7-C10-C19	-57.3	-50.6	-52.9	-60.1	-53.7	-55.3	-57.3	-50.8	-52.9
C8-C7-C2-C1	-43.6	-38.1	-40.2	-42.9	-37.4	-39.5	-43.6	-37.8	-40.2
D									
C7-C8-C11-C12	-112.1	-76.2	-73.2	117.9	113.8	116.8	-112.1	-76.2	-73.2
C8-C7-C10-C19	-68.2	-63.6	-64.1	-116.5	-57.1	-55.9	-117.5	-63.6	-64.0
C8-C7-C2-C1	-66.1	-47.2	-47.0	-117.1	-49.6	-48.9	-125.6	-46.9	-47.0
C7-C8-C9-C20	-83.4	-48.9	-49.1	-99.3	-55.3	-54.6	-119.4	-48.3	-49.1
E									
C7-C8-C11-C12	113.8	115.8	116.3	-106.2	-74.2	-73.7	113.8	115.8	116.3
C8-C7-C10-C19	-66.7	-58.8	-57.1	-71.8	-63.9	-64.8	-112.8	-58.6	-57.1
C8-C7-C2-C1	-54.9	-47.5	-47.9	-61.4	-45.6	-46.1	-119.9	-47.6	-48.0
C7-C8-C9-C20	-63.3	-56.1	-54.7	-81.0	-49.6	-49.4	-100.2	-55.8	-54.9

Supplementary information Table 3: Ingress/egress channels found in x-ray structures PDB ID: 2J0D, 2V0M and 3NXU.

x-ray	channel	2a	2b	2e	2f	4	5	Solvent
2J0D	3		2b	2e				S
2V0M	4	2a	2b			4		S
3NXU	3		2b		2f			S